MARTIN MARIETTA ENERGY SYSTEMS LIBRARIES
3 4456 0050629 0

ORNL-TM-5140

Cy 62

Evaluation of Thermal Response in Fort St. Vrain Reactor Primary System to a Design Basis Depressurization Accident Followed by Cooling with Two Pelton Wheel Drives Operating at 7000 rpm

J. P. Sanders
W. D. Turner
S. J. Ball
R. M. DeVault
G. E. Giles
D. D. Paul

OAK RIDGE NATIONAL LABORATORY
CENTRAL RESEARCH LIBRARY
DOCUMENT COLLECTION
LIBRARY LOAN COPY
DO NOT TRANSFER TO ANOTHER PERSON
If you wish someone else to see this document, send in name with document and the library will arrange a loan.
UCN-7969
(3 3-67)

OAK RIDGE NATIONAL LABORATORY
OPERATED BY UNION CARBIDE CORPORATION • FOR THE U.S. ATOMIC ENERGY COMMISSION

Printed in the United States of America. Available from
National Technical Information Service
U.S. Department of Commerce
5285 Port Royal Road, Springfield, Virginia 22161
Price: Printed Copy $5.50; Microfiche $2.25

This report was prepared as an account of work sponsored by the United States Government. Neither the United States nor the Energy Research and Development Administration, nor any of their employees, nor any of their contractors, subcontractors, or their employees, makes any warranty, express or implied, or assumes any legal liability or responsibility for the accuracy, completeness or usefulness of any information, apparatus, product or process disclosed, or represents that its use would not infringe privately owned rights.

ORNL-TM-5140

Contract No. W-7405-eng-26

Reactor Division

EVALUATION OF THERMAL RESPONSE IN FORT ST. VRAIN REACTOR PRIMARY SYSTEM TO A DESIGN BASIS DEPRESSURIZATION ACCIDENT FOLLOWED BY COOLING WITH TWO PELTON WHEEL DRIVES OPERATING AT 7000 RPM

J. P. Sanders R. M. DeVault
W. D. Turner G. E. Giles
S. J. Ball D. D. Paul

Work performed for the U.S. Nuclear Regulatory Commission under Interagency Agreement 40-494-75.

DECEMBER 1975

NOTICE: This document contains information of a preliminary nature and was prepared primarily for internal use at the Oak Ridge National Laboratory. It is subject to revision or correction and therefore does not represent a final report.

OAK RIDGE NATIONAL LABORATORY
Oak Ridge, Tennessee 37830
operated by
UNION CARBIDE CORPORATION
for the
U.S. ENERGY RESEARCH AND DEVELOPMENT ADMINISTRATION

MARTIN MARIETTA ENERGY SYSTEMS LIBRARIES
3 4456 0050629 0

CONTENTS

FOREWORD v

ABSTRACT 1

INTRODUCTION 1

CIRCULATOR AND STEAM GENERATOR PERFORMANCE 4

Circulator Performance Evaluation 4

Steam Generator Model Description 6

Results 10

DEVELOPMENT OF THE FLODIS CODE 14

THERMAL ANALYSIS OF THE FORT ST. VRAIN CORE 17

CONCLUSIONS 35

APPENDIX. SIMULATION OF THE FSV DBDA USING THE ORECA CODE 37

REFERENCES 42

FOREWORD

This work was initiated under a technical assistance assignment from the Gas-Cooled Reactors Branch (GCRB) of the Division of Reactor Licensing, USNRC. This work followed from a general task involving both the specific evaluation of certain aspects of high temperature gas-cooled reactor (HTGR) thermal response during abnormal operation and the development of general computer programs for these and associated tasks.

As of July 1, 1975, the task assignment was transferred to the Division of Technical Review, USNRC, and work has continued as an ad hoc request from that Division.

Associated tasks have been executed at ORNL under the sponsorship of the Division of Reactor Safety Research, USNRC. One of these tasks has included the evaluation of computational methods used by the General Atomic Company (GAC) for system analysis under abnormal conditions. This has led to the development of computer codes that emulate, at least in part, the computational procedures described by GAC. The detailed information about this particular transient provided the opportunity to compare the computed values from the ORNL programs with the tabulated results provided by GAC. As a result, as much of the transient as possible has been evaluated using these programs developed at ORNL under Reactor Safety Research (RSR) support. The results of these calculations are presented in the appendix of this report.

The major difference between the computer programs developed at ORNL under the two programs is that for the licensing effort, choices have been made that will indicate "conservative" values for the important system variables. The programs developed for the RSR study have been directed toward the prediction of the most probable values, which can be compared with operating experience for the Fort St. Vrain reactor.

EVALUATION OF THERMAL RESPONSE IN FORT ST. VRAIN REACTOR PRIMARY SYSTEM TO A DESIGN BASIS DEPRESSURIZATION ACCIDENT FOLLOWED BY COOLING WITH TWO PELTON WHEEL DRIVES OPERATING AT 7000 RPM

J. P. Sanders W. D. Turner *
S. J. Ball R. M. DeVault *
G. E. Giles * D. D. Paul

ABSTRACT

Independent computations have been performed at ORNL to determine the thermal and hydraulic response of the primary system of the Fort St. Vrain reactor to a specified design basis depressurization accident (DBDA). For this accident it is stated that two of the four auxiliary drives on the circulators start operating at 7000 rpm after a 5-min delay. Detailed tabulations describing this response were provided by the vendor, General Atomic Company (GAC). The calculations at ORNL supported the values given for primary system flow and pressure loss, and they confirmed the heat removal capacity of the flooded steam generators. The fuel and outlet helium temperatures calculated by ORNL generally reached higher values during the transient due to the fact that the ORNL calculations were performed using a single-channel calculation that could not include the effect of interregional heat conduction. An ORNL code that is developmental, but which includes interregional conduction, agrees well with the GAC values. The results of these calculations are presented graphically.

Key words: Gas coolant, conduction, convection, computer program, safety analysis.

INTRODUCTION

During the operation of the Fort St. Vrain reactor primary system prior to licensing the reactor for operation at power, the Pelton wheel drives on the main circulators were used to provide helium flow. Inspection of these drives following this operating period indicated some granular cracking. As a result, the original cast Pelton wheels were replaced with forgings, and, on the basis of harmonic analysis, a request was made to change the technical specifications to require operation at 7000 rpm rather than 10,550 rpm, which had been specified previously.

---

*Members of Computer Science Division, UCCND

In a letter[1] dated January 6, 1975, the Gas-Cooled Reactors Branch (GCRB) of the Directorate of Licensing (presently, the Division of Reactor Licensing — DRL) asked a series of questions related to this change and associated matters. A response[2] was made by the Public Service Company (PSC) of Colorado on January 16, 1975. In Fig. 14.11-3-1 of this response, the fuel and gas temperatures were presented as a function of time following a rapid depressurization accident with startup of two of the circulators in one loop, operating at 7000 rpm with a 5-min delay. ORNL, as a consultant to the GCRB, was asked to make an independent evaluation of the temperatures given in this plot.

To facilitate this evaluation task, detailed questions were presented by the GCRB in a letter[3] dated February 7, 1975. The response from PSC was provided in tabulations accompanying a letter[4] dated February 28, 1975. The tabulations presented as numerical listings both the information presented graphically in the previous letter and intermediate values of temperatures in the primary circuit plus certain requested geometric information.

A preliminary evaluation was provided by ORNL to the GCRB in a letter[5] dated March 21, 1975. The results were made available to PSC on May 12, 1975, and a review meeting was held in Washington on June 20 including staff members of the GCRB, ORNL, PSC, and the General Atomic Company (GAC), which is the vendor for the Fort St. Vrain nuclear steam supply system. The conclusions of PSC and GAC were summarized and presented in a letter[6] dated July 8, 1975.

As a consequence of the meeting on June 20, it became apparent that the maximum fuel temperature, which had been one of the major items of interest during the ORNL evaluation, was not going to be the limiting criterion during the accident sequence. ORNL was asked to modify its calculations to produce a more realistic estimate of the exit temperature from the highest power refueling region. This was done by increasing the ratio of graphite to fuel in the "unit cell" or "single channel" model used by ORNL to represent the ratio of graphite to fuel in an entire refueling region. The results would still be conservative due to the fact that interregional conduction is not represented in the ORNL model.

During this period, refinements were made in the computer program used by ORNL to evaluate the distribution of flow among the various refueling regions during the transient. In addition, a program written at ORNL under sponsorship of the Division of Reactor Safety Research (RSR) was used to evaluate the temperatures in the FSV core. This program, which is designated ORECA, is modeled on the general formulation that is presented for the RECA program written by GAC. The ORECA program is currently in a developmental stage, and one of the major objectives in performing these calculations was to evaluate the functions of the ORECA program in comparison with the RECA program. At present, only the core of the reactor is represented in the ORECA calculations.

The following report is divided into three sections. In the first section, those calculations concerning the performance of the circulator and the steam generator (as a heat removal unit) are described, and the results are presented. In the second section, a short description of the FLODIS calculation is given; this calculation determines the distribution of coolant among the various refueling regions during the transient. Finally, in the third section, the results of the single channel and the modified single channel calculations are given; both the maximum outlet coolant temperatures and the maximum fuel temperatures resulting from this calculation are presented.

In the appendix of this report, the results of the ORECA calculations are given for comparison purposes.

CIRCULATOR AND STEAM GENERATOR PERFORMANCE

G. E. Giles R. M. DeVault

Circulator Performance Evaluation

The main circulator performance during accident conditions was investigated for the transient described in the response[4] to question 14.11-4. The circulator performance was taken as depicted in Fig. 3-1 of Gulf-GA-A10349 (Ref. 7). A copy of this figure with the apparent system line is included in this report (Fig. 1).

By using the temperatures and gas flow rates in the response and assuming the circulator turns at 7000 rpm, the corrected flow rates and mass flow rates are calculated. The compressor map given by General Atomic can be reduced to a single compressor speed curve using similarity parameters if the circulator is assumed to operate as an ideal compressor (i.e., no viscous losses, etc.).

Similarity parameters.

$$\frac{\phi/\phi_0}{N} = \text{constant} , \tag{1}$$

$$\frac{\Psi/\Psi_0}{N^2} = \text{constant} , \tag{2}$$

where

N = circulator speed, rpm,

ΔP = pressure rise across circulator,

ϕ/ϕ_0 = corrected mass flow rate/design mass flow rate,

$\Psi/\Psi_0 = \Delta P/P \big/ (\Delta P/P)_{design}$.

The pressure drop for a particular corrected speed and mass flow rate can be calculated from this information, if the pressure drops and flow rates for a constant corrected speed line are known. To evaluate this technique, the 9550 speed curve was extrapolated to the other speeds

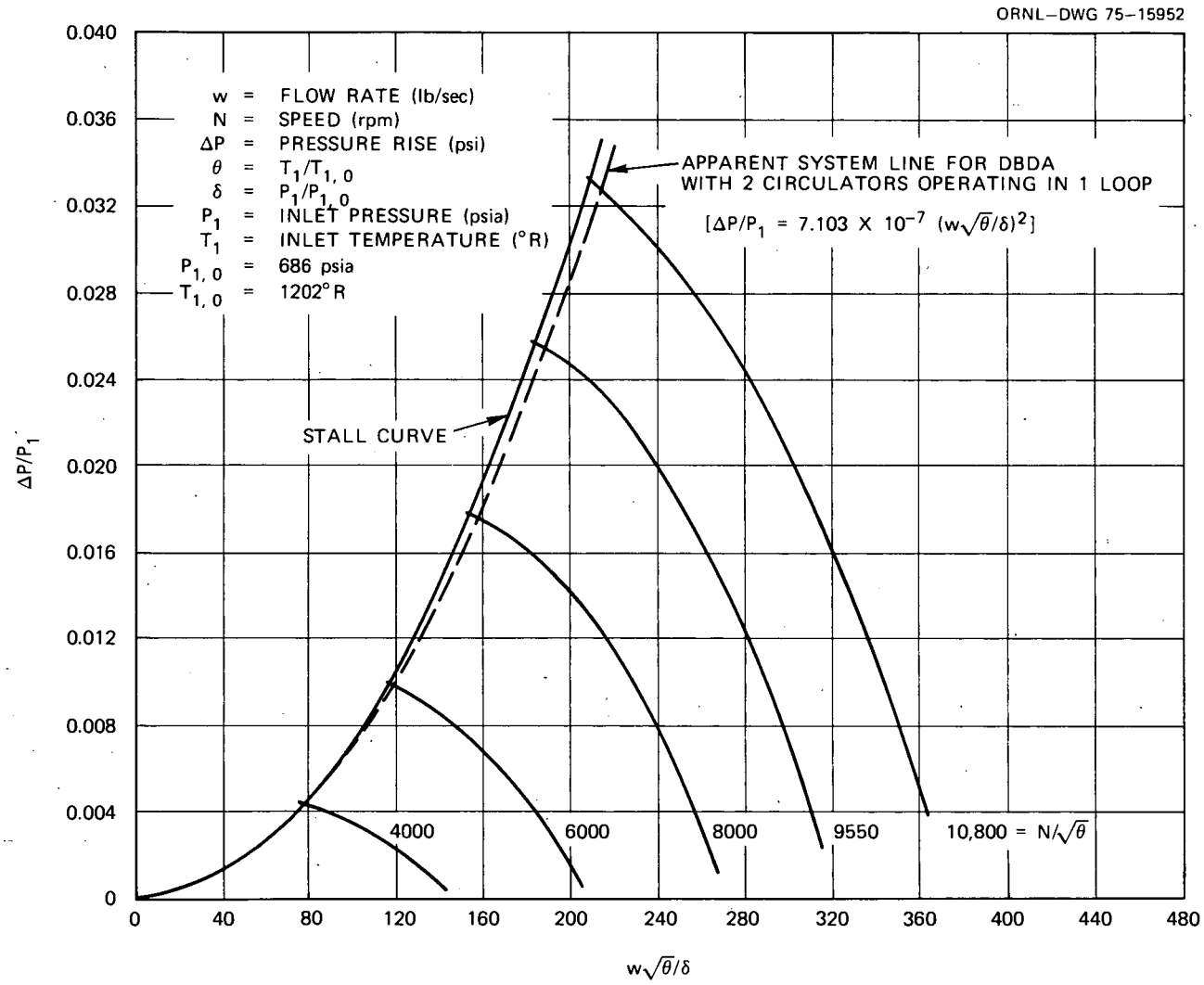

Fig. 1. Circulator characteristic curves and apparent system operating line for the DBDA for the Fort St. Vrain reactor.

and compared with those curves in the compressor map. The agreement was very close; and, therefore, the similarity approach could be used with confidence if the compressor map shown was derived from experimental data.

By using the similarity technique and the data in the response, the pressure drop can be calculated and plotted on the compressor map. This was the manner in which the apparent system line was deduced.

The reason for using the similarity technique was to force the circulator performance calculations to maintain a speed of 7000 rpm without stating in advance what the system line was for the particular case to be analyzed. The pressure head of the circulator calculated in this manner compares favorably with the loop pressure drops presented in the response and shows that the circulator (if it were ideal) would deliver substantially more pressure head than required (Fig. 2). Analysis of the viscous losses was not included. The maximum torque required during this transient was 51 ft-lb.

Steam Generator Model Description

Upon leaving the reactor core, the primary coolant of the Fort St. Vrain HTGR flows first through a reheater, then into superheater 2, and finally into the steam generator. The steam generator consists of three sections. The sections, as they are encountered by the primary coolant, are: (1) superheater 1, (2) the evaporator, and (3) the economizer. The flow is countercurrent in all the heat exchangers with the exception of superheater 2, which has parallel flow.

In developing a model of the heat transfer system, provisions had to be made for the varying physical characteristics of each heat exchanger. This was best done by developing a model which divided the steam generator into three distinct sections. The model neglected the reheater since the secondary flow through the reheater is negligible after the depressurization transient has decayed.

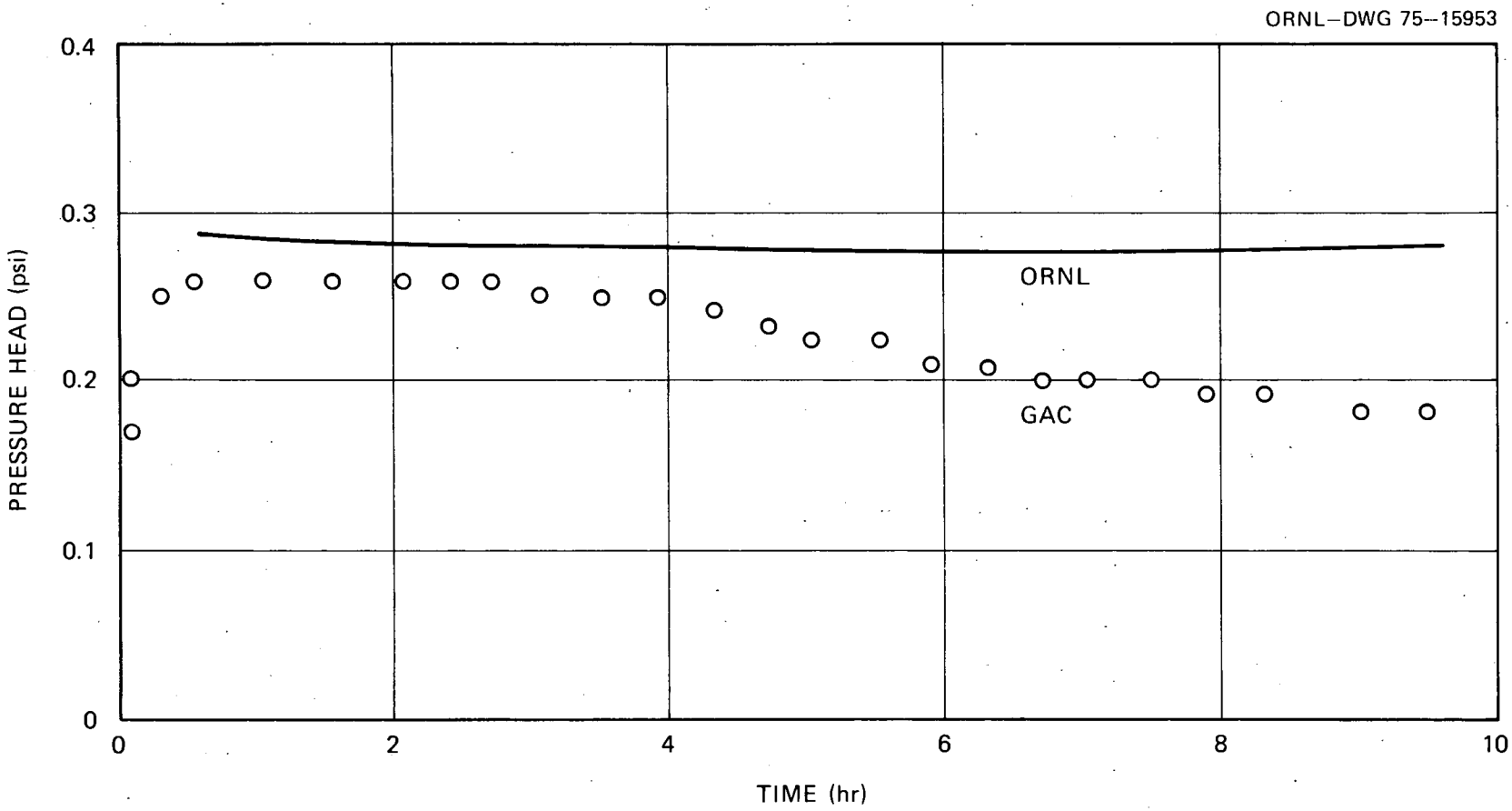

Fig. 2. Pressure head required for the loop during the Fort St. Vrain DBDA.

The TUBE Program calculates the coefficients C and N which are used in obtaining the Nusselt number (N_{Nu}) , i.e.,

$$N_{Nu} = C_1 (C_G)(N_{Re})^n , \tag{3}$$

where

C_G = adjustment to Grimison correlation due to the number of rows considered,

N_{Re} = Reynolds number.

Subroutine TUBE obtains the Nusselt number coefficient, C_1, from a method based on an extension of the tabulated values given by McAdams.[8] A method using the best fit to the statistical trend was used to provide the necessary equations and constants to calculate the Nusselt number coefficients. Subroutine TUBE stores these constants and uses the relationships to obtain the Nusselt number coefficients. If the transverse or longitudinal pitches are not represented by the statistical equations, the subroutine uses an interpolation procedure to obtain those constants necessary for determining the Nusselt number coefficients. The coefficient is divided by the Prandtl number to the one-third power, so that the correlation can be applied to gases with other Prandtl numbers.

The model incorporated the physical characteristics that are shown in Table 1. From the physical descriptions given in Table 1, the Nusselt number calculated for the steam generator was

$$N_{Nu} = 0.5702\ N_{Re}^{0.5633}\ N_{Pr}^{1/3} . \tag{4}$$

The Nusselt number correlation calculated for superheater 2 was

$$N_{Nu} = 0.5578\ N_{Re}^{0.5645}\ N_{Pr}^{1/3} . \tag{5}$$

Each of the four exchanger sections was divided up into five subsections to improve both accuracy and convergence. The iterative procedure used was to guess at the outlet water temperature at superheater 1 and back-calculate the inlet water temperature to the economizer. The heat exchanger calculations were assumed to converge when the calculated value was within a sufficiently small tolerance of the known value.

Table 1. Steam generator and reheater physical characteristics

Part I	Single module data		
	EES	SH2	RH
A. Effective heat transfer area without leads, ft^2			
Installed	2480	850	440
Ideal	2120	704	388
B. Superficial gas flow area, ft^2. Area occupied by:	18.634	15.569	18.201
Tubing	11.657	9.367	11.636
Support structure	0.435	0.420	0.442
C. Effective transverse tube spacing (pitch), in.	1.42	1.48	1.575
D. Effective longitudinal tube spacing (pitch), in.	1.47	1.44	1.575
E. Tube outside diameter, in.	1.00	1.00	1.125
F. Tube wall thickness, in.	.138/.138/.225	0.205	0.140
G. Tube material	SA-213 T2/T22/T22	SB-163-GR2 NI-FE-CR	SB-163-GR2 NI-FE-CR
H. Effective tube length, ft			
Installed	175.0	60.0	17.8
Ideal[a]	149.99[a]	49.81	15.7
I. Cross-sectional free flow area, ft^2	6.542	5.782	6.123

[a]Ideal economizer length, ft = 76.81
Ideal evaporator 1 length, ft = 25.51
Ideal evaporator 2 length, ft = 23.38
Ideal superheater 1 length, ft = 24.29
Total 149.99

Division of EES installed surface not readily available. Recommend using same percentage division as for ideal if needed for analysis.

Results

As shown in Figs. 3 through 5, the computed heat duty and helium exit temperature compare favorably with those reported in the response. These results are essentially independent of the helium heat transfer coefficient since the helium flow rate is so small that the helium reaches the feed water temperature well before the end of the heat exchanger is reached. The response indicated that the helium temperature at the core inlet was lower than the feed water temperature due to the gas flowing over the PCRV thermal barrier which is cooled by 140°F water. This effect was not included in this analysis, since the major helium temperature change was in the heat exchanger.

The only area of significant disagreement appeared in the first 0.1 hr of the transient where the calculated heat duty is much greater than the value tabulated by the General Atomic Company. This is apparently due to the fact that the ORNL program uses a pseudotransient technique of driving the steady-state solution with transient parameters (i.e., flow and temperature). If the steam generator is slow in responding to changes, then the heat duty will be less than these calculations indicate. Only a small portion of the transient and only a total duty of 4.4×10^5 Btu difference in total heat transferred ($\sim$0.5% of total transferred) is involved. This difference is considered insignificant.

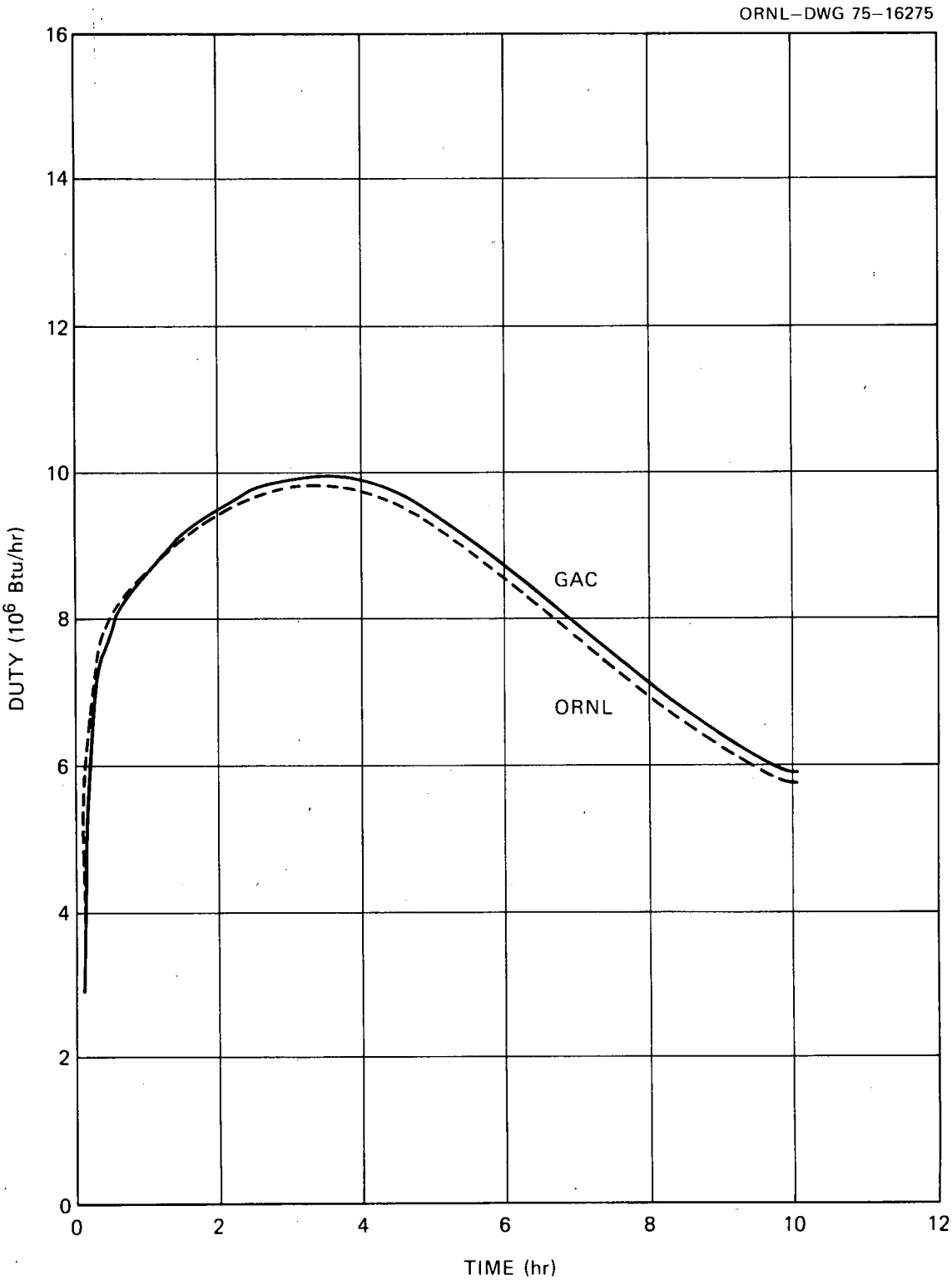

Fig. 3. Heat removal rate in the steam generators of the Fort St. Vrain reactor during the DBDA.

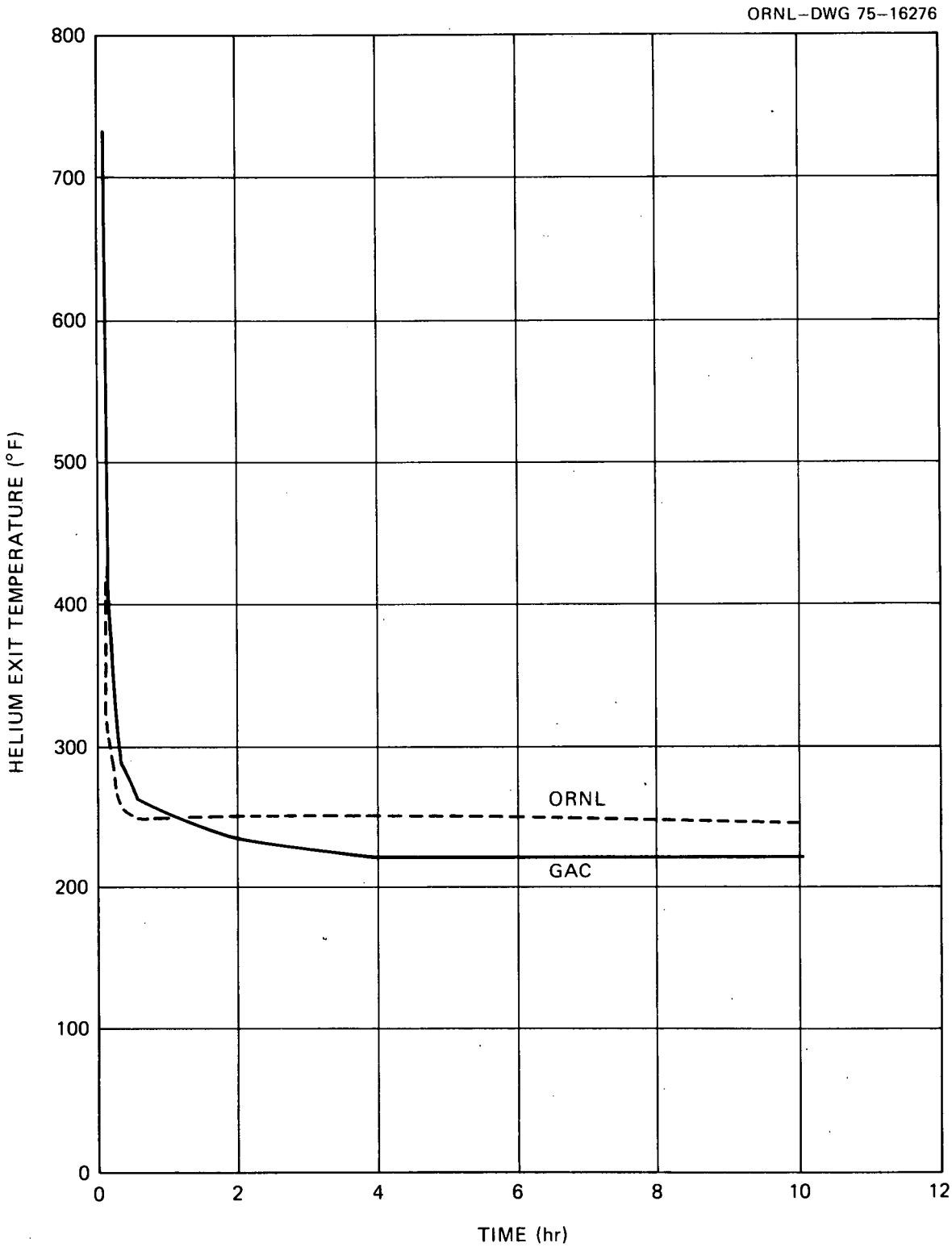

Fig. 4. Helium exit temperature from the steam generators during the Fort St. Vrain DBDA.

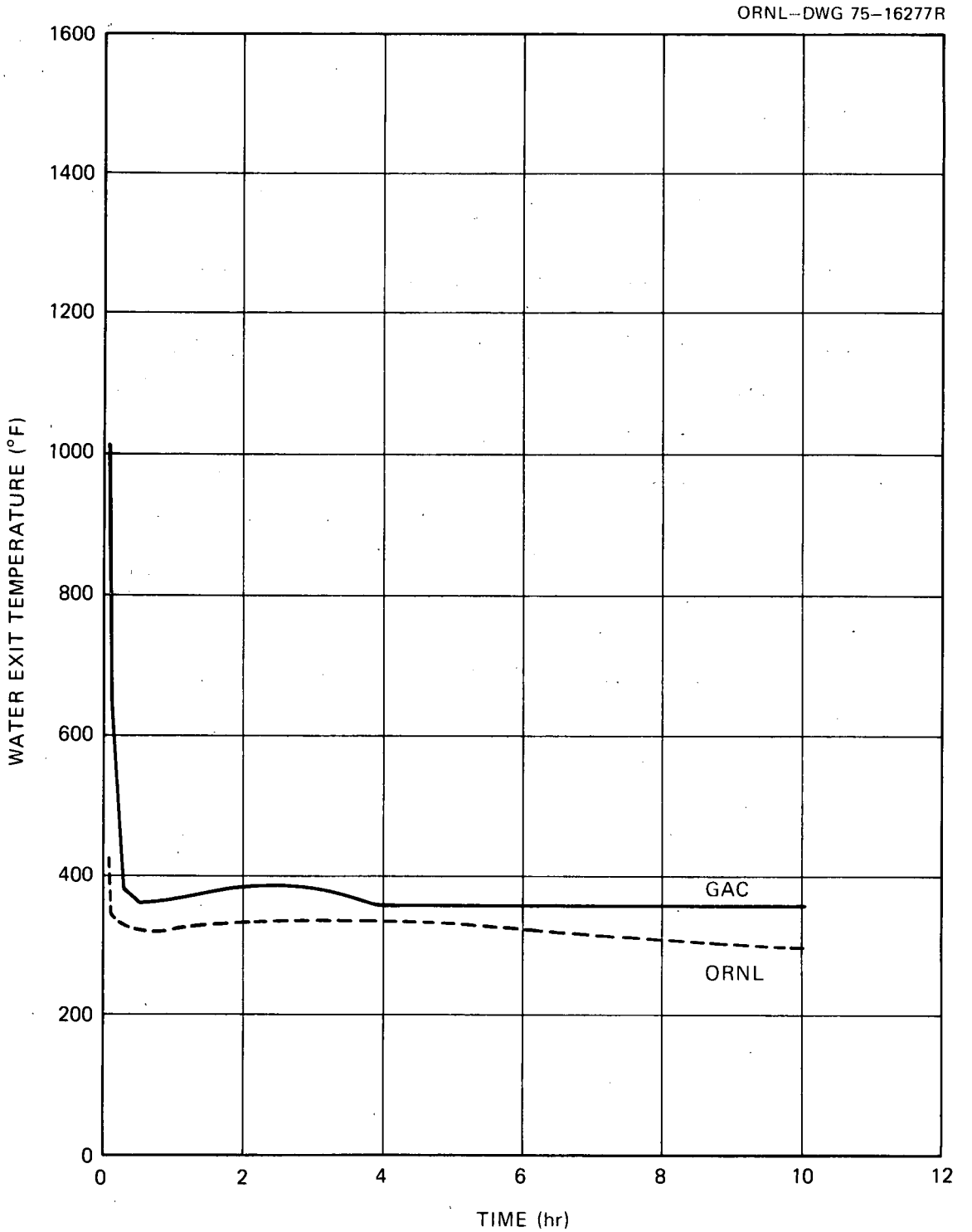

Fig. 5. Water exit temperature from the steam generators during the Fort St. Vrain DBDA.

DEVELOPMENT OF THE FLODIS CODE

D. D. Paul

A lumped parameter model, FLODIS, of the Fort St. Vrain reactor core was developed. This analysis was done to supplement the study of emergency core cooling at reduced flow rates produced by the modification of the Pelton wheel operating specifications. The code calculates the coolant flow redistribution following a design basis depressurization accident and was developed to supply the CCCM code with region flow rates as a function of time. A preliminary version of the code is operational.

Development of the FLODIS code required capabilities for calculating core temperatures, fluid temperatures, and the flow distribution. These parameters are not independent of each other. An iteration scheme was devised where each one of these parameters could be calculated assuming the other two parameters were known. The iteration scheme converged when the assumed value for each parameter was within some small convergence criteria of the calculated value.

Since the distribution of the total flow was of primary interest, a detailed temperature distribution in the core was not necessary. Thus, a simplified core model was chosen which has only one node per refueling region.

Figure 6 shows preliminary results of the single node per refueling region model. Normalized flow is plotted versus time for the hottest channel in the Fort St. Vrain reactor. The normalized flow is defined as

$$W_{norm} = \frac{W_i}{W_{avg}} , \tag{6}$$

where

W_i = flow rate in region i,

W_{avg} = average flow = total flow divided by the total number of fuel columns times the number of fuel columns in region i.

At steady-state conditions, the hot channel normalized flow should be equal to the radial peaking factor. When flow resumes after the 5-min adiabatic heatup, the hot channel normalized flow drops to less than 1.2.

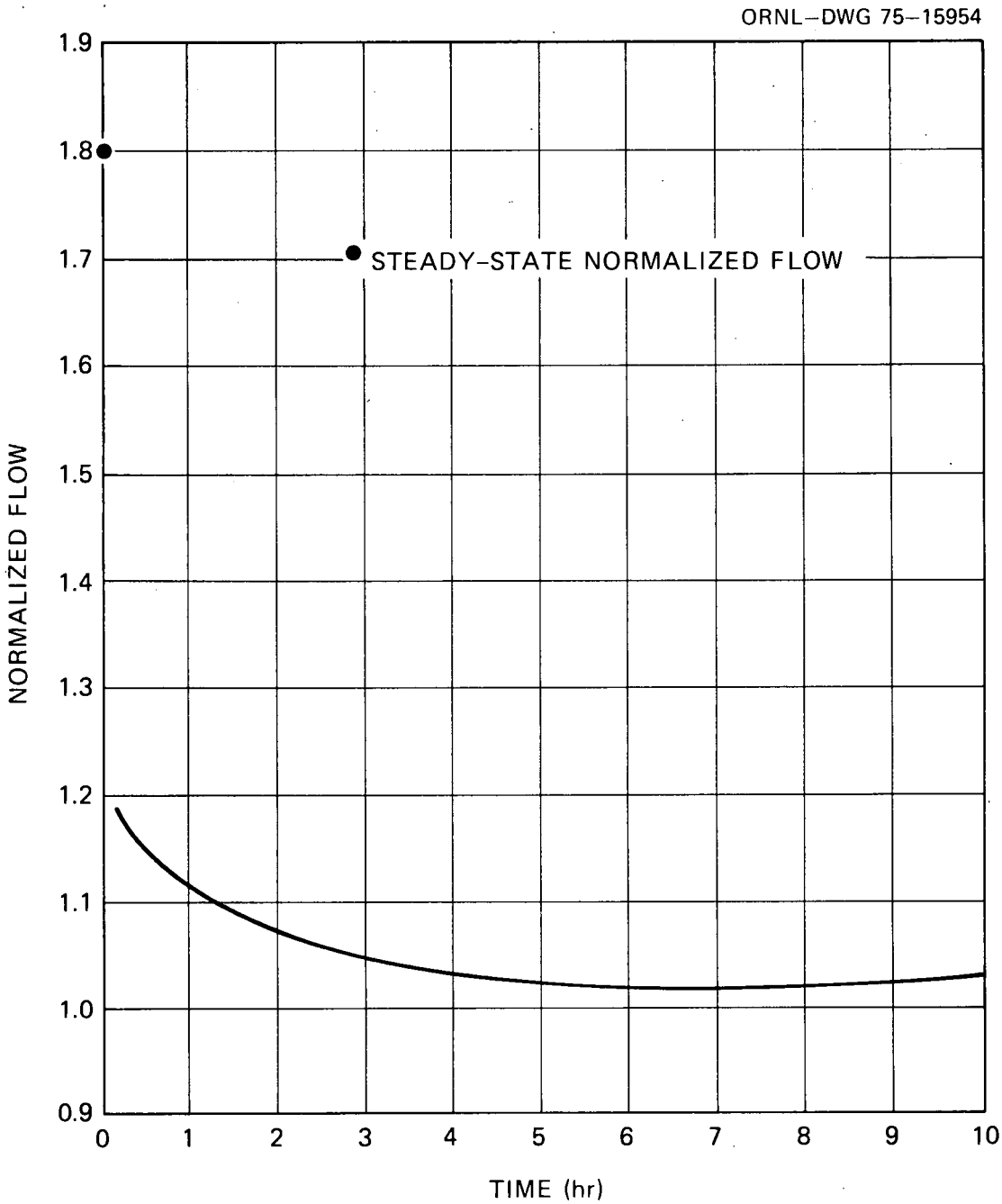

Fig. 6. Normalized flow calculated by the FLODIS code for the hottest refueling region in the Fort St. Vrain core following the DBDA.

During the transient, the hot channel does not cool as fast as the other channels, and therefore, the normalized flow continues to decrease due primarily to feedback effects of temperature in calculating frictional losses. However, once the hot channel begins to cool down, the gradients between refueling regions start to collapse and the normalized flow in the hot channel slowly increases.

These normalized flows were used as input to the CCCM code to obtain a detailed temperature distribution.

THERMAL ANALYSIS OF THE FORT ST. VRAIN CORE

W. D. Turner

In response to a request from the Division of Reactor Licensing (DRL) of NRC, a thermal analysis was made on the active core of the Fort St. Vrain HTGR to determine the maximum fuel and coolant exit temperatures following a specified design basis depressurization accident (DBDA) followed by operation with two circulators at 7000 rpm. This analysis was done to evaluate similar calculations performed by the General Atomic Company (GAC).

The thermal analysis was completed using the coupled-conduction convection model (CCCM) computer code[9–11] which was especially designed for this type of calculation. The model using CCCM consisted of a unit cell which included one fuel rod, the surrounding graphite moderator and half of a coolant channel. The unit cell was totally insulated from the remainder of the core except for the influence from the coolant flow. Thus, there was no radial flow of heat to adjoining refueling regions. The unit cell is depicted in Fig. 7. The thermal properties used in the analysis are listed in Table 2.

The thermal conductivity of 10 Btu/hr-ft-°F that was used for the graphite yields both a conservative maximum fuel temperature and maximum coolant exit temperature. A conductivity of 20 Btu/hr-ft-°F was used in a study of the influence of various parameters, and the calculation indicated values for both the fuel and coolant exit temperature which were lower by about 20°F. This results from the fact that the controlling resistance to the flow of heat from the fuel to the coolant is the resistance of the gas film.

Since the coolant exit temperatures were of prime importance, the ratio of heat capacity of graphite to that of fuel in a refueling region should be correctly simulated in the unit cell. The ratio of graphite volume to fuel volume in the active core of a refueling region was 1.38 times that in the unit cell. Thus, the density of the material in the zone marked GRAPHITE 1 (Fig. 7) was increased by 38%. The ratio of graphite volume to coolant volume in the reflector elements of a refueling region were 1.25 times the corresponding ratio in the unit cell. Likewise,

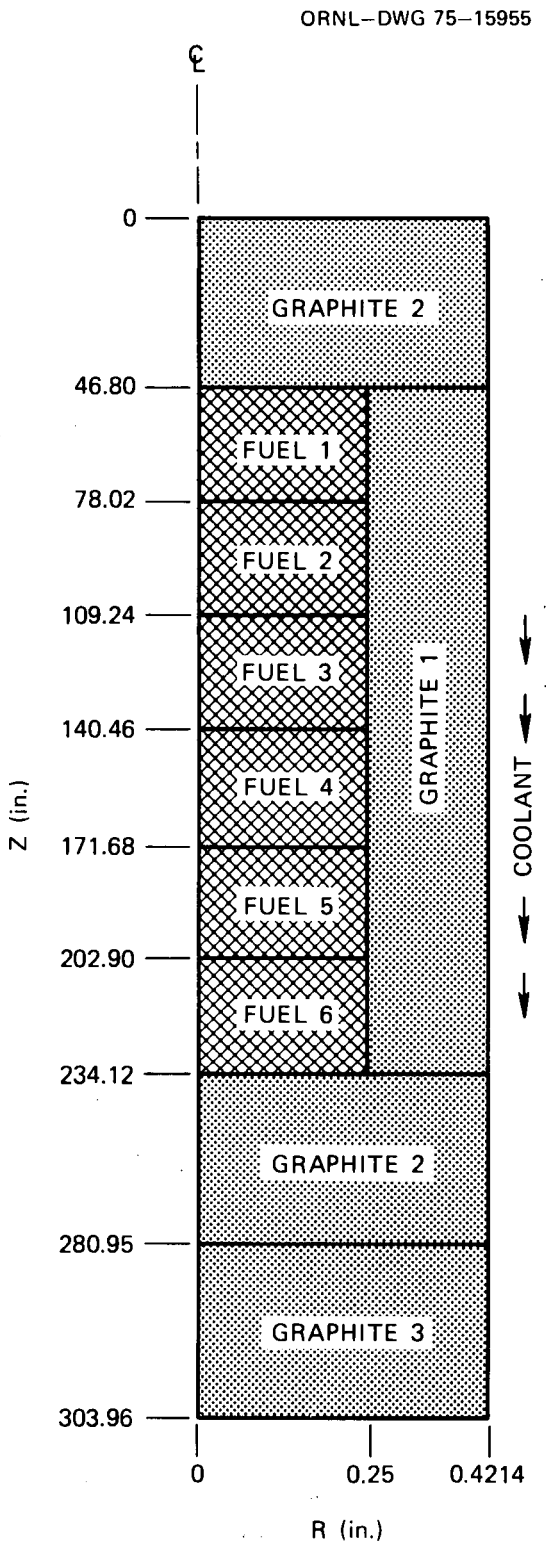

Fig. 7. Two-dimensional unit cell in the active core of the Fort St. Vrain reactor during normal operation and for reduced coolant flow.

Table 2. Basic thermal properties of materials used in unit cell

---

Fuel

$k = 4.0$ Btu/hr-ft-°F (Sec. 4.4.2.2.1c, Ref. 12)

$\rho Cp(T) = 3.38 + 2.74 \times 10^{-2}T - 4.88 \times 10^{-6}T^2 - 1.46 \times 10^5/T^2$ Btu/ft^3-°F

Note: T is in °R (Sec. 3.6.3.1, Ref. 13) .

Graphite

$k = 10.0$ Btu/hr-ft-°F (Sec. 5.1.2, Ref. 14)

$\rho = 107$ lb/ft^3 (Table D.2-15, Ref. 13)

$Cp(T) = -0.103 + 6.472 \times 10^{-4}T - 2.667 \times 10^{-7}T^2 + 3.97 \times 10^{-11}T^3$ Btu/lb-°F

Note: T is in °R (Sec. 3.6.3.1, Ref. 13)

---

the ratio of graphite volume to coolant volume in the core support block of a refueling region was 1.17 times the corresponding ratio in the unit cell. Thus, the densities of the materials in the zones marked GRAPHITE 2 and GRAPHITE 3, Fig. 7, were increased by 25% and 17%, respectively.

The material properties for the coolant are presented in Table 3.

The following boundary conditions were applied to the model shown in Fig. 7. At the top of the unit cell, heat was transferred to the coolant by convection and to the superstructure above the active core by radiation. However, the total heat flow across this boundary was so small that an insulated boundary would have yielded the same results. The bottom of the cylinder and the boundary along r=0 were considered to be no-flux surfaces. Heat was transferred between the outer surface of the graphite and the coolant by forced convection. The heat transfer coefficient was determined by the flow regime of the coolant. The flow was assumed to be turbulent for Reynolds numbers exceeding 4000 and laminar for Reynolds numbers less then 2100.

The unit cell model assumed that the 0.625-in.-diam coolant channel extended through the core support block unaltered. Actually, the 0.625-in.-diam channels merged into one 7.55-in.-diam coolant channel per fuel element in the bottom of the lower reflectors. Then, these channels merged into one 21-in.-diam channel in the core support block. These larger channels involved a greatly reduced surface area for heat flow between the coolant and graphite. The net result was that the model allowed a much larger flow of heat between the coolant and graphite in the

Table 3. Material properties of coolant used in unit cell[15]

Thermal Conductivity

$k(P,T) = A(P) + B(P)T + C(P)T^2$ Btu/hr-ft-°F

where P is in psia, T is in °F, and the coefficients A, B and C are defined below.

Pressure(psia)	A	$B \times 10^5$	$C \times 10^8$
14.7	0.0809175	9.9936	−1.10025
100.0	0.0834957	10.0842	−1.13598
1000.0	0.0863791	10.1611	−1.20405

Density

$\rho(P,T) = 0.37303\ P/T$ lb/ft^3 ,

where P is in psia and T is in °R.

Specific Heat

$Cp = 1.2425$ Btu/lb-°F .

Viscosity

$\mu(T) = 6.7 \times 10^{-4} T^{0.68}$ lb/hr-ft .

Pressure

$$P(t) = \begin{cases} 688 \text{ psia for time} = 0 \\ 12 \text{ psia for time} > 0 \ . \end{cases}$$

lower reflector and core support block than actually existed. Thus, the heat flow from the coolant to the graphite was corrected in the following manner. In the zone 275.25 in. < z ≤ 288.95 in., the mass velocity, G, was calculated by assuming that the coolant from one-hundred-and-two 0.625-in.-diam channels and six 0.5-in.-diam channels was collected into one 7.55-in.-diam channel (Sec. 3.4.1 of Ref. 13 and engineering drawings from Ref. 16). The heat transfer coefficient was then calculated based on this mass velocity and the larger coolant channel diameter. Then, the heat flow was determined, based on this heat transfer coefficient, and the surface area of the larger channel. Since this heat flow between coolant and graphite corresponded to an entire fuel element, it had to be adjusted for the unit cell. This was done by dividing it by twice 105.84, since there were that many unit cells (each including half of a coolant channel) per regular

fuel element. A similar analysis was made in the zone 288.95 in. < z $\leq$ 303.96 in. For this calculation the total heat transferred between the coolant and graphite was divided by twice 690.24 since this represented the number of unit cells per refueling region.

During normal operating conditions, the coolant flow through the unit cell was determined as follows. The total core mass flow was 3.6667 $\times 10^6$ lb/hr (Ref. 17), and the flow area of the coolant channels in the active core was 51.0 ft^2 (Table 3.6.-1 of Ref. 13). With the assumption of 3.5% bypass flow (Ref. 17), the average mass velocity in a refueling region for unrestricted flow was 6.938×10^4 lb/hr-ft^2.

The coolant mass velocity as a function of time was taken from the FLODIS code for the refueling region of interest. The version of FLODIS which provided the coolant mass velocity used only one lumped axial node per refueling region. FLODIS used as input the total flow of coolant as a function of time as given by GAC for this DBDA. The time function for the coolant mass velocity, provided by FLODIS for the refueling region with a radial power peaking factor of 1.7843, is shown in Table 4.

The power density in the fuel zone of the unit cell was calculated as follows (Sec. 3.4.1.1 of Ref. 13). There were 210 columns composed of six regular fuel elements in the active core, and each element contained 210 fuel sticks which were 29.5 in. long. There were 37 columns composed of six control fuel elements where each element contained 120 fuel sticks. The fuel sticks in the first five elements were 29.5 in. long and the sixth was only 21.7 in. in length. Since the diameter of each fuel stick was 0.5 in., the total volume of the fuel in the active core was

$$V_f = \pi(0.5/2)^2\{(210)(210)(6)(29.5) + (37)(120)[(5)(29.5) + 21.7]\} \quad (7)$$

or

$$V_f = 1.68015 \times 10^6 \text{ in}^3 \text{ or } 27532 \text{ liters.} \quad (8)$$

The average power density in the fuel was then 31.9 kW/liter based on a power of 878.3 MW(t) which was the stated power level at 105% power (Ref. 17). In order to simulate the axial power distribution in a fuel element, each fuel zone depicted in Fig. 7 was related to an axial power peaking factor as shown in Table 5.

Table 4. Time-dependent coolant mass velocity following DBDA with 5-min delay for refueling region with radial power peaking factor of 1.7843 as calculated by FLODIS

Time (hr)	Factor ($lb/hr \cdot ft^2$)
0.0	1.1978×10^5
0.0^+	0.0
0.08299	0.0
0.0833	396.06
0.09922	477.36
0.11	530.41
0.12	582.13
0.13	593.41
0.15	601.46
0.20	610.00
0.30	620.94
0.40	628.66
0.50	633.29
1.0	629.10
1.5	623.09
2.0	616.13
2.5	614.58
3.0	611.59
3.5	609.17
4.0	608.36
4.5	605.69
5.0	603.30
5.5	601.60
7.0	599.97
10.0	608.30

Table 5. Axial power peaking factors[4]

Zone	Factor
Fuel 1	0.8205
Fuel 2	1.1498
Fuel 3	1.3269
Fuel 4	1.0787
Fuel 5	0.9096
Fuel 6	0.7145

Let $\dot{q}'''(t,r,z)$ represent the power density at time t in refueling region r at axial location z. Then, the power density was calculated as

$$\dot{q}'''(t,r,z) = \hat{q} \cdot P_r \cdot P_z \cdot f(t) \ , \tag{9}$$

where

$\hat{q}$ = the average power density,

P_r = the radial power peaking factor for the refueling region of interest,

P_z = the axial power peaking factor at position z,

and

$$f(t) = 0.128(t + 3.796 \times 10^{-4})^{-0.261} \ , \tag{10}$$

where t is in seconds (Eq. 5.10 of Ref. 14).

Each case run on CCCM involved a steady-state analysis to obtain the normal operating temperatures followed by a transient analysis involving the DBDA. In each case, the reactor was assumed to be operating at 105% power initially. The inlet helium temperature was assumed to be 773°F (Table 3.1-1 of Ref. 13). At the start of an accident, the flow of helium stopped, the pressure dropped from 688.0 to 12.0 psia (Ref. 17), and the reactor was scrammed with the power decaying with time according to the relationship shown in Eq.(5). After five minutes, the coolant flow was restarted and the inlet temperature followed the GAC-supplied curve shown in Table 6.

The maximum coolant exit temperature as calculated by the model which has just been described is plotted as a function of time in Fig. 8. This corresponded to the average coolant exit temperature from the refueling region with a radial power peaking factor of 1.7843 which was the highest powered region in the Fort St. Vrain HTGR during the specified accident. Note that the peak temperature was 2411°F and occurred 4 hr after the accident. This corresponded to a maximum of 2000°F at about 3.75 hr as calculated by GAC.[4]

Figure 9 depicts the coolant exit temperature as a function of time for a nominal (radial power factor equal to unity) refueling region. The mass velocity to the unit cell was based on the total mass flow to the active core, as supplied by GAC, divided by the total flow area of the

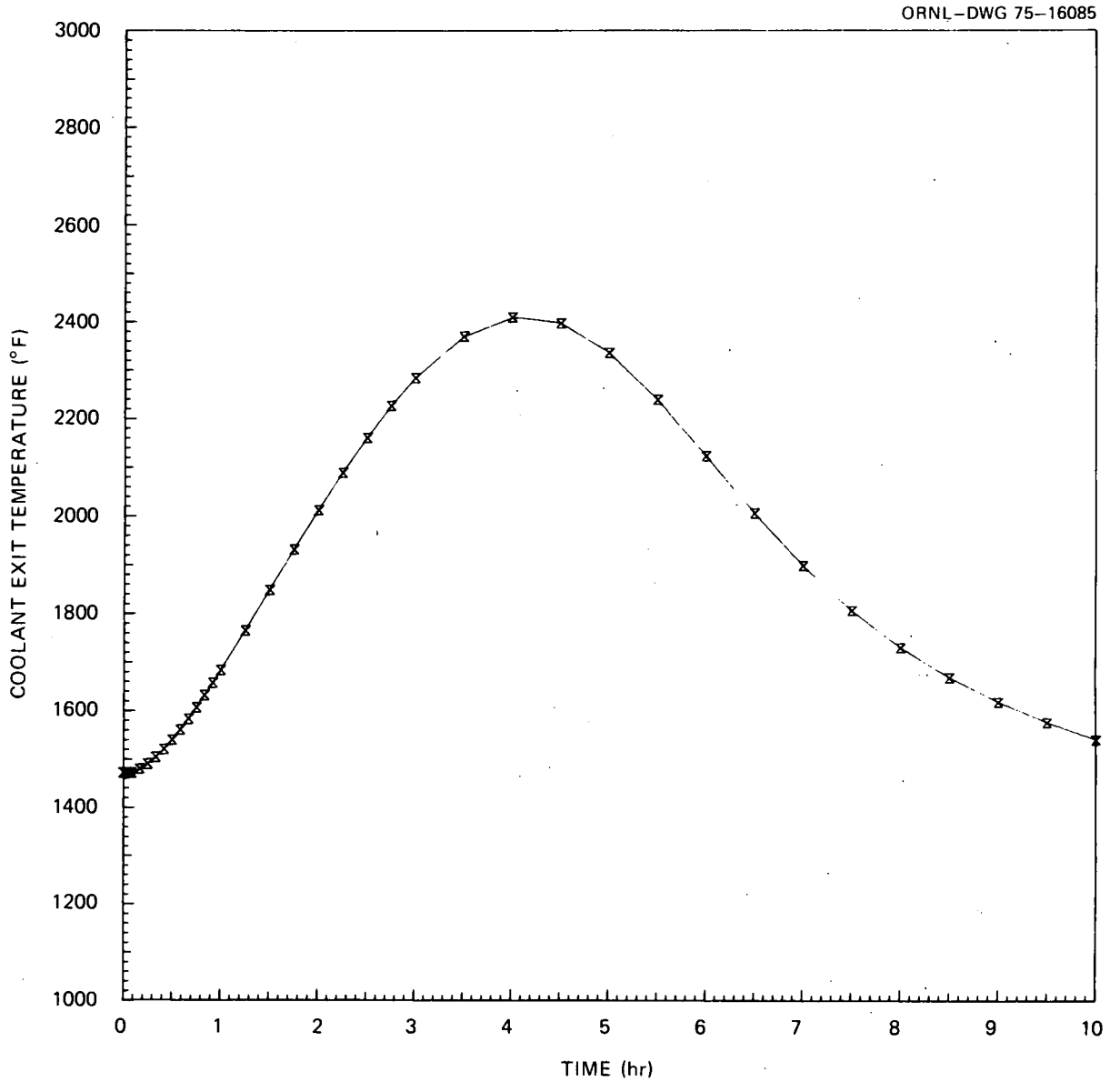

Fig. 8. Coolant exit temperature from the highest power refueling region of the Fort St. Vrain reactor, for the DBDA followed by operation of two circulators at 7000 rpm after a 5-min delay.

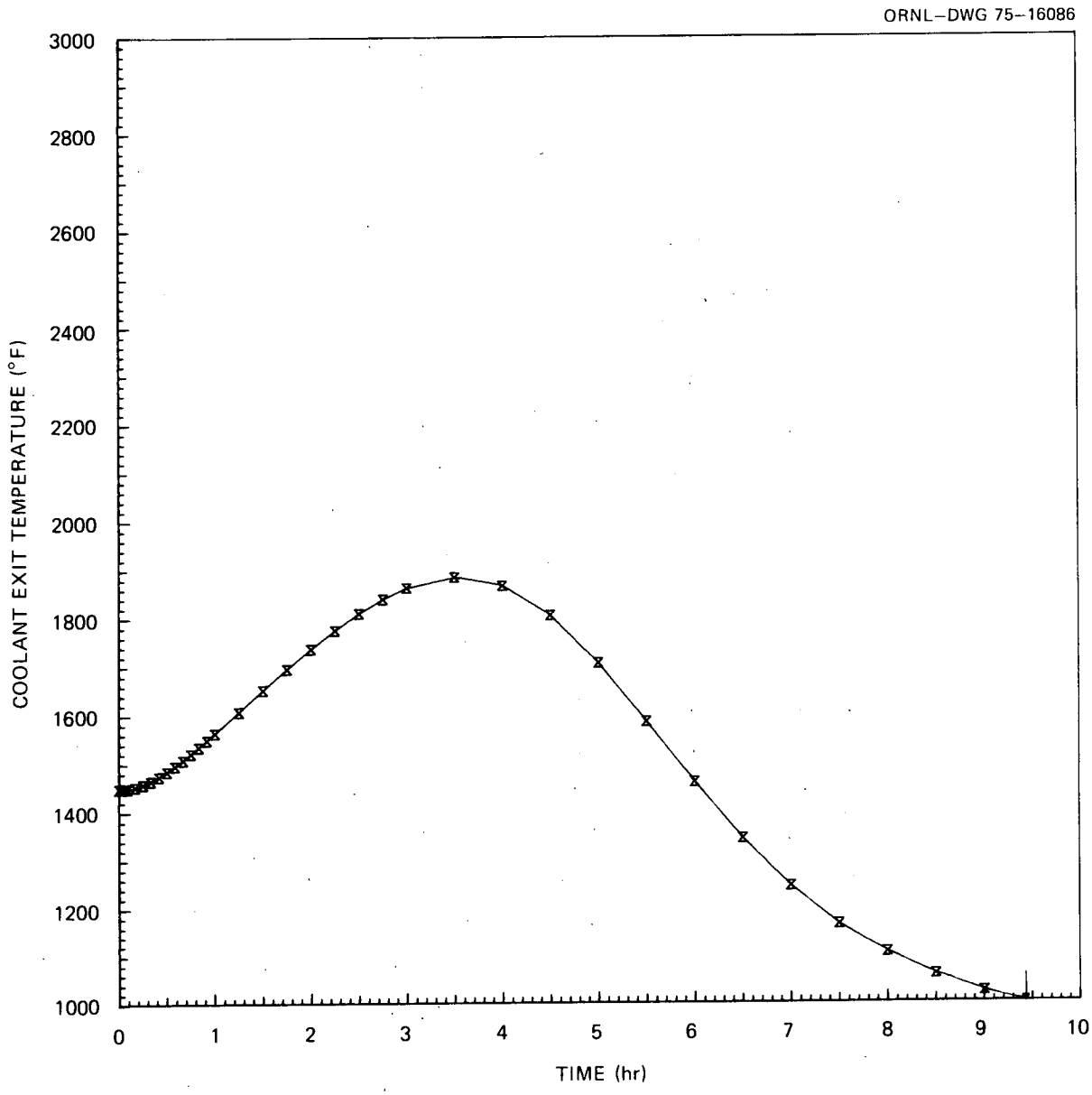

Fig. 9. Average coolant exit temperature from the active core of the Fort St. Vrain reactor following the specified DBDA.

Table 6. Inlet temperature as a function of time for DBDA followed by operation with two circulators at 7000 rpm, 5-min delay[4]

Time (hr)	Temperature (°F)
0	773
0^+	773
0.0832	773
0.0833	734
0.1032	419
0.2953	290
0.5442	262
1.0409	249
1.5089	242
2.0309	235
2.4309	231
2.7509	229
3.1509	226
3.5509	224
3.9509	221
4.3509	220
10.0309	220

active core assuming a bypass flow of 3.5%. The time function is shown in Table 7. This calculation yielded a peak temperature of 1886°F at 3.5 hr after the accident. This temperature should be representative of the average coolant temperature as it exited from the active core. The maximum value of the average coolant exit temperature reported by GAC[4] was 1757°F at 3.15 hr after the accident.

A parametric study was made to determine the circulator speed required to insure that the coolant exit temperatures remained under 2000°F. It was assumed that the percentage of total flow to each refueling region remained constant with increased total flow. The CCCM calculations for the highest powered refueling region were repeated by assuming that the two circulators were operating at speeds up to 14,000 rpm. All data remained the same except for the mass velocity which was changed by the same ratio of the circulator speed. These calculations were repeated for the model yielding the average core outlet temperature. The maximum coolant exit temperatures are plotted as a function of time in Fig. 10 for the

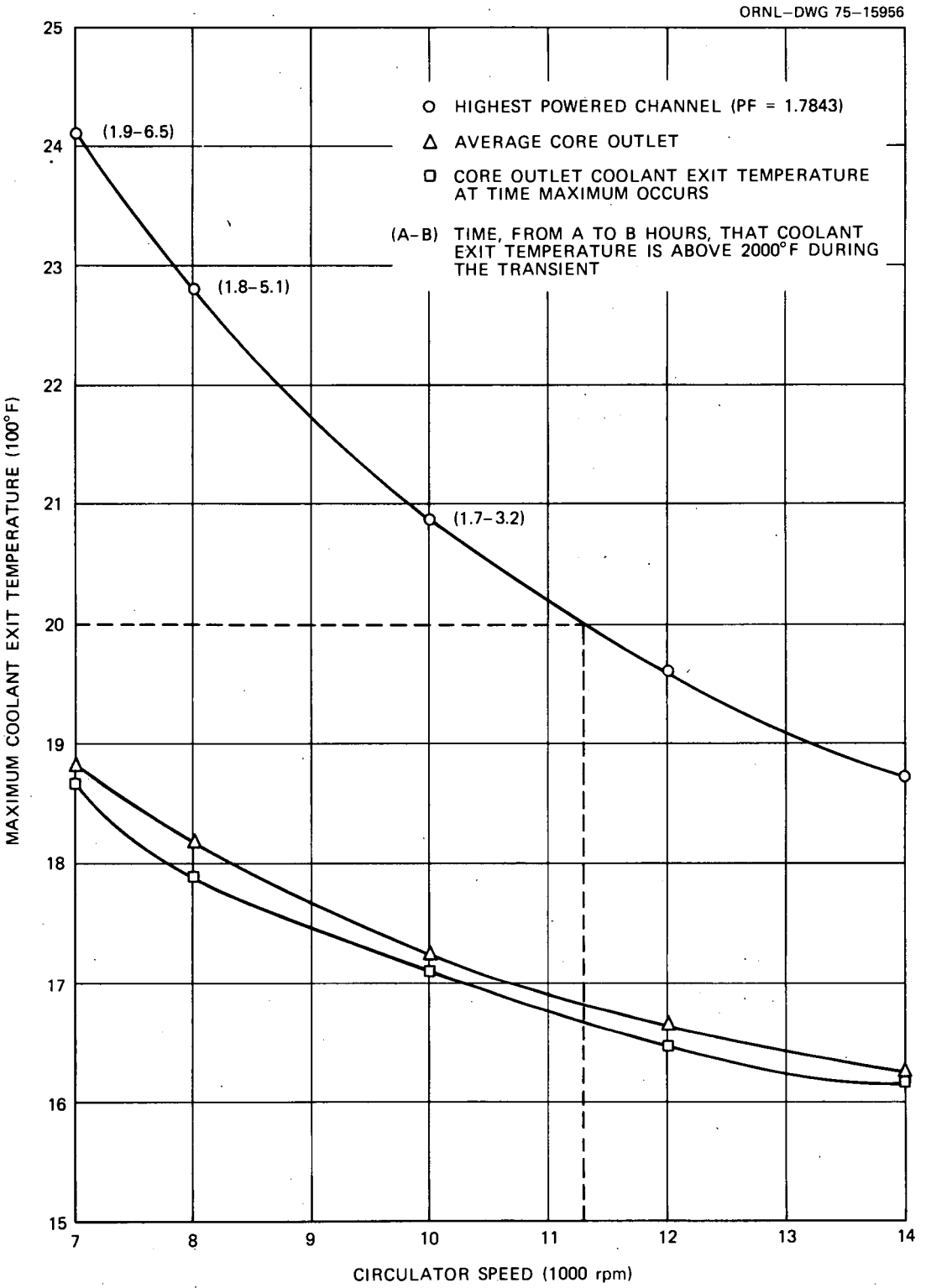

Fig. 10. Maximum coolant exit temperature reached during the transient for the highest power refueling region and the average core outlet temperatures as a function of circulator speed.

Table 7. Time-dependent coolant mass velocity following DBDA with 5-min delay for refueling region based on average flow to active core as supplied by GAC[4]

Time (hr)	Factor ($lb/hr \cdot ft^2$)
0.0	6.9377×10^4
0.0+	0.0
0.08299	0.0
0.0833	342.04
0.12	501.62
0.2455	534.22
0.5028	564.06
1.0009	575.16
1.5089	582.10
2.0909	586.95
2.5109	591.12
3.0309	593.89
3.5109	596.67
4.0309	599.44
4.1509	600.14

refueling region with radial power peaking factor of 1.7843 and for the average core outlet case. The bottom curve, Fig. 10, represents the coolant exit temperatures as a function of circulator speed for the average core outlet model at the times when the maximum temperatures occurred in the highest powered refueling region (shown in top curve). The values in parentheses alongside the top curve indicate the time during the transient, measured in hours after the accident, when the coolant exit temperature exceeded 2000°F. Within the limitations of the model, these curves indicate that a circulator speed of 11,300 rpm must be maintained to insure a maximum coolant exit temperature below 2000°F.

In order to determine the maximum fuel temperature during the transient following the DBDA, the original model that was described was executed using CCCM without adjusting the density of the graphite zones to reflect the actual ratio of graphite to fuel in a refueling region. The maximum fuel temperature is plotted as a function of time in Fig. 11. The maximum fuel temperature was 2618°F and occurred at 2.75 hr after initiation of the DBDA.

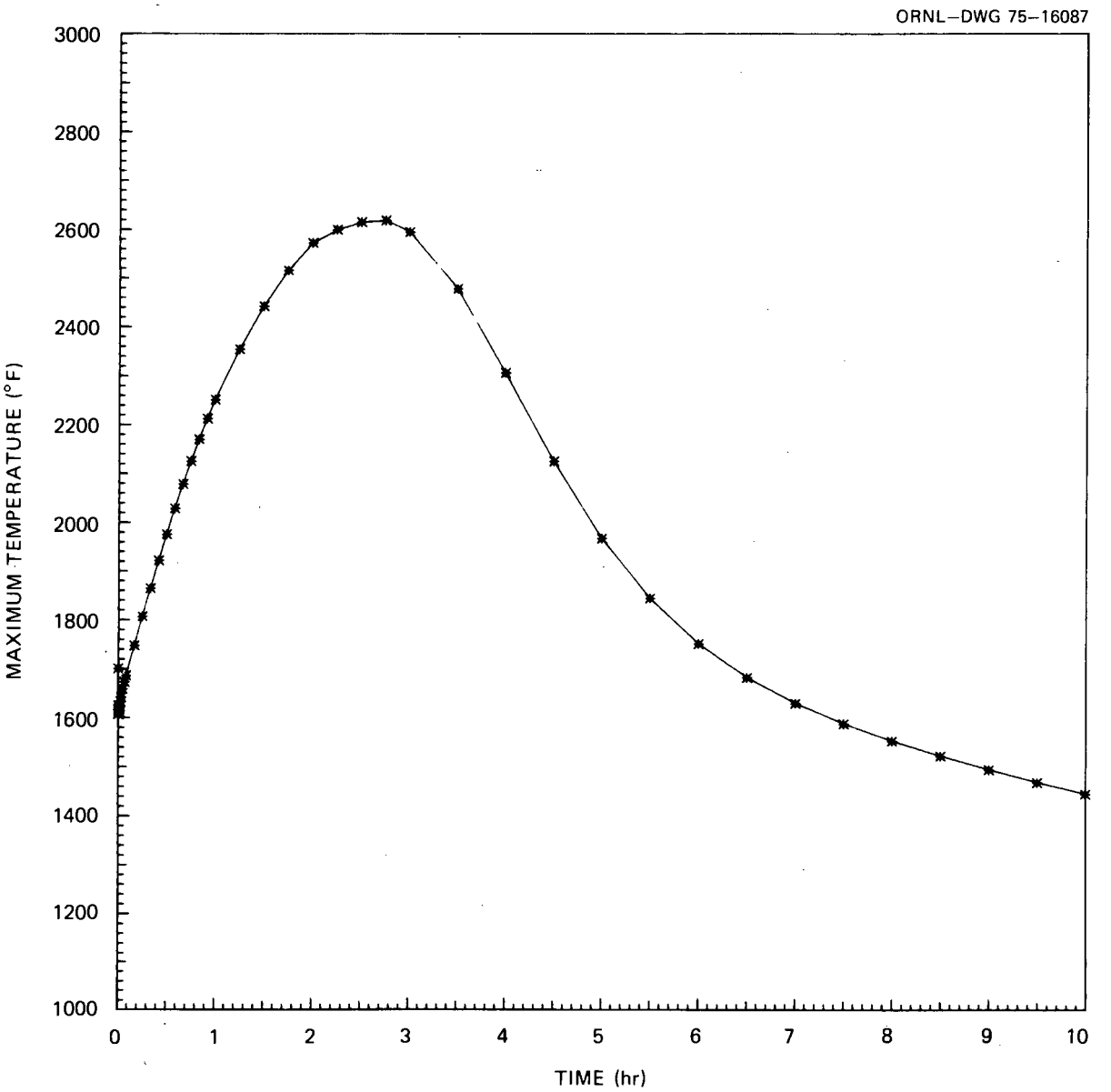

Fig. 11. Maximum fuel temperature in the highest power refueling region of the Fort St. Vrain reactor following the specified DBDA.

Figures 12 through 15 show axial temperature profiles through the center of the fuel and through the coolant channel during normal operation, at the time of maximum fuel temperature, at the time of maximum coolant exit temperature, and at 10 hr after start of the accident.

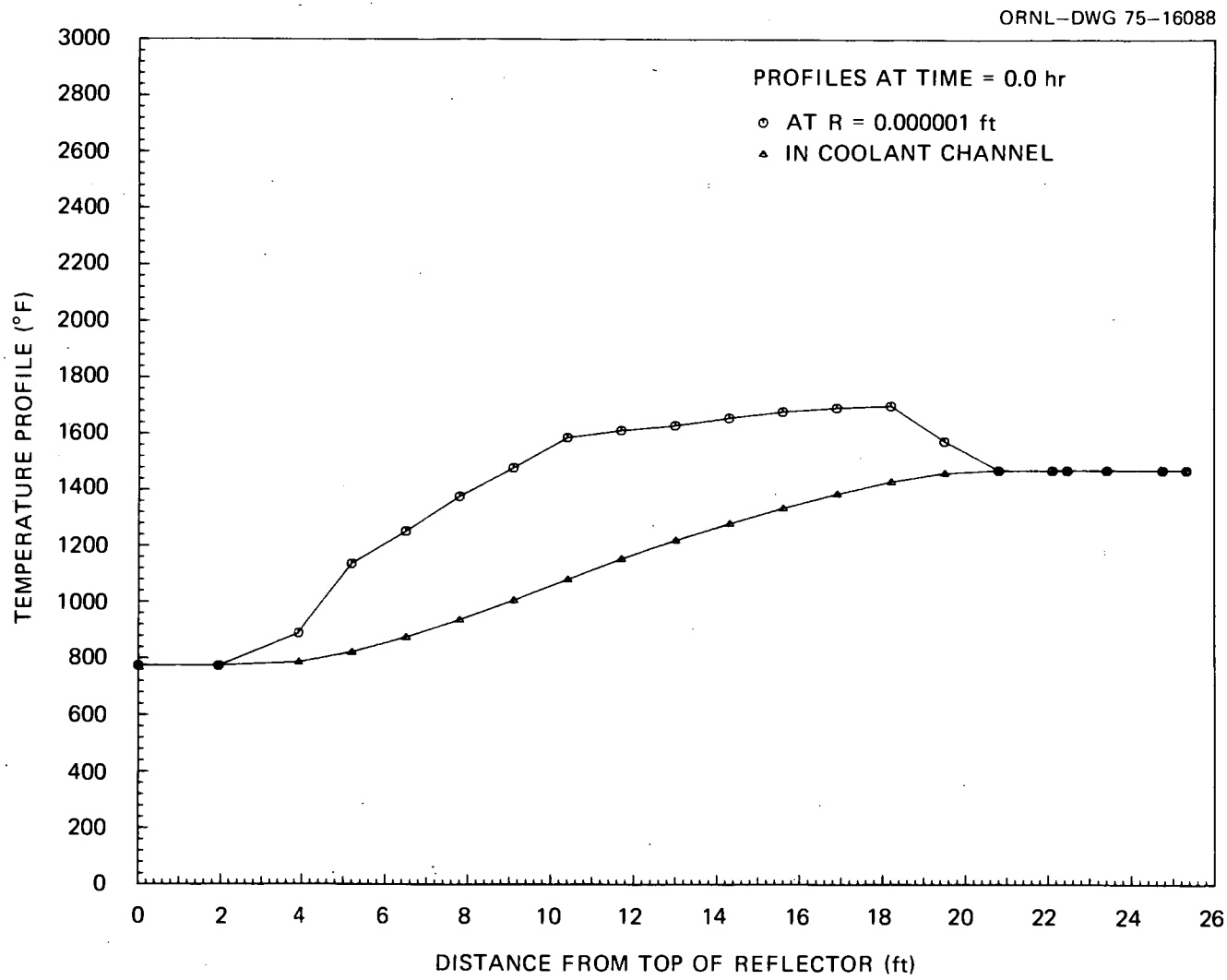

Fig. 12. Fuel and coolant profiles at normal operating conditions in the highest power refueling region of the Fort St. Vrain reactor.

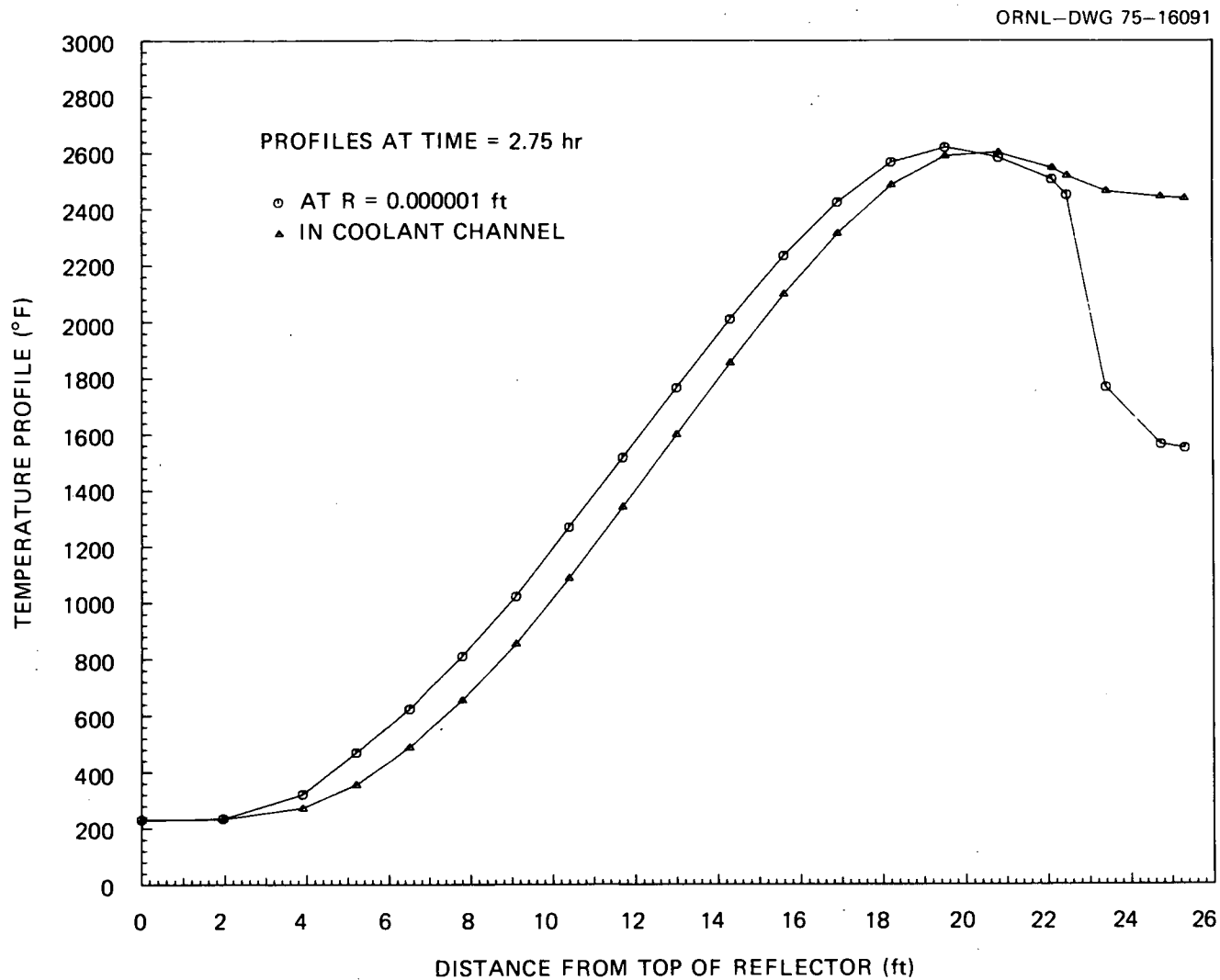

Fig. 13. Fuel and coolant profiles at the time of maximum fuel temperature in the highest power refueling region of the Fort St. Vrain reactor following the specified DBDA.

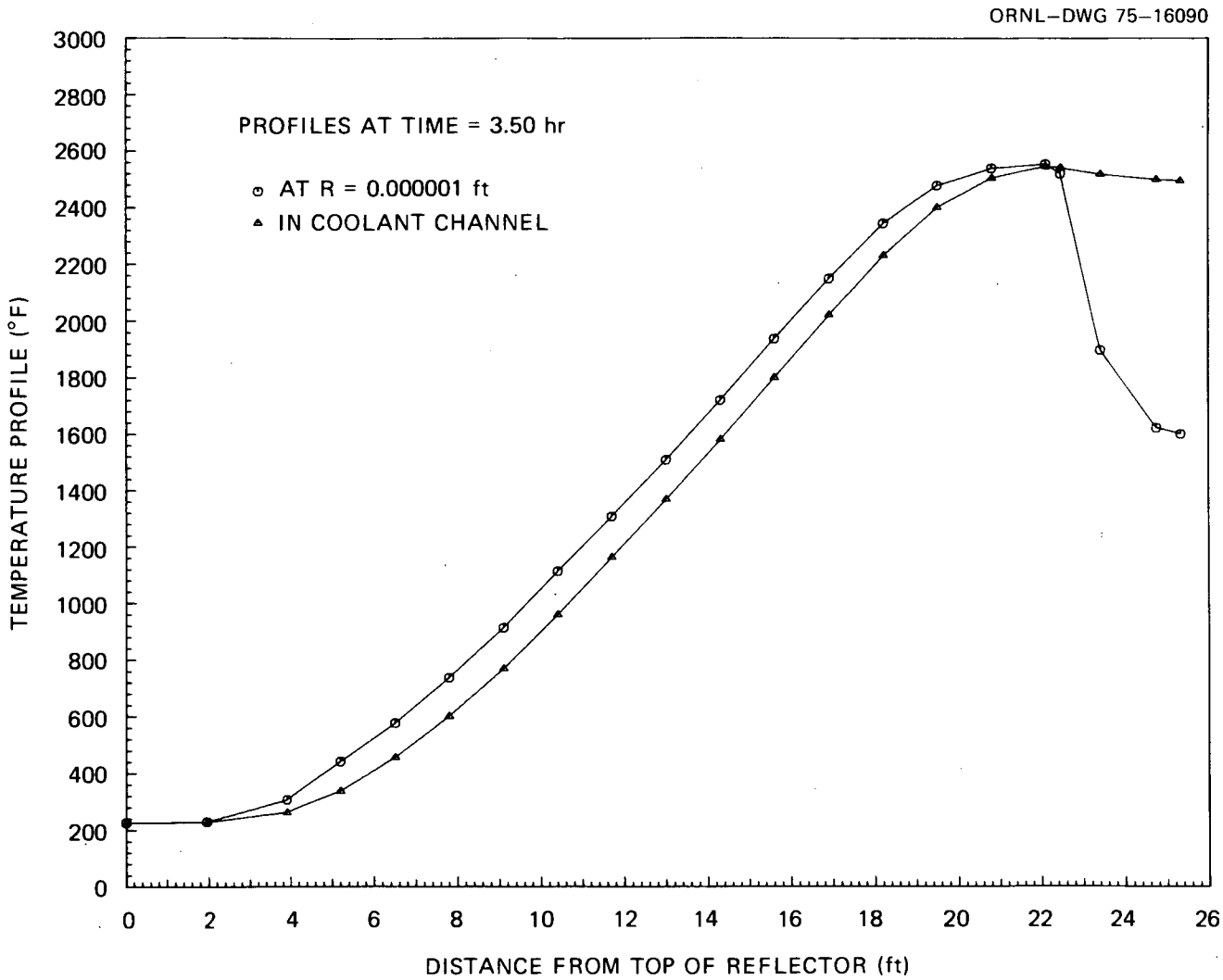

Fig. 14. Fuel and coolant profiles at the time of maximum coolant exit temperature in the highest power refueling region of the Fort St. Vrain reactor following the specified DBDA.

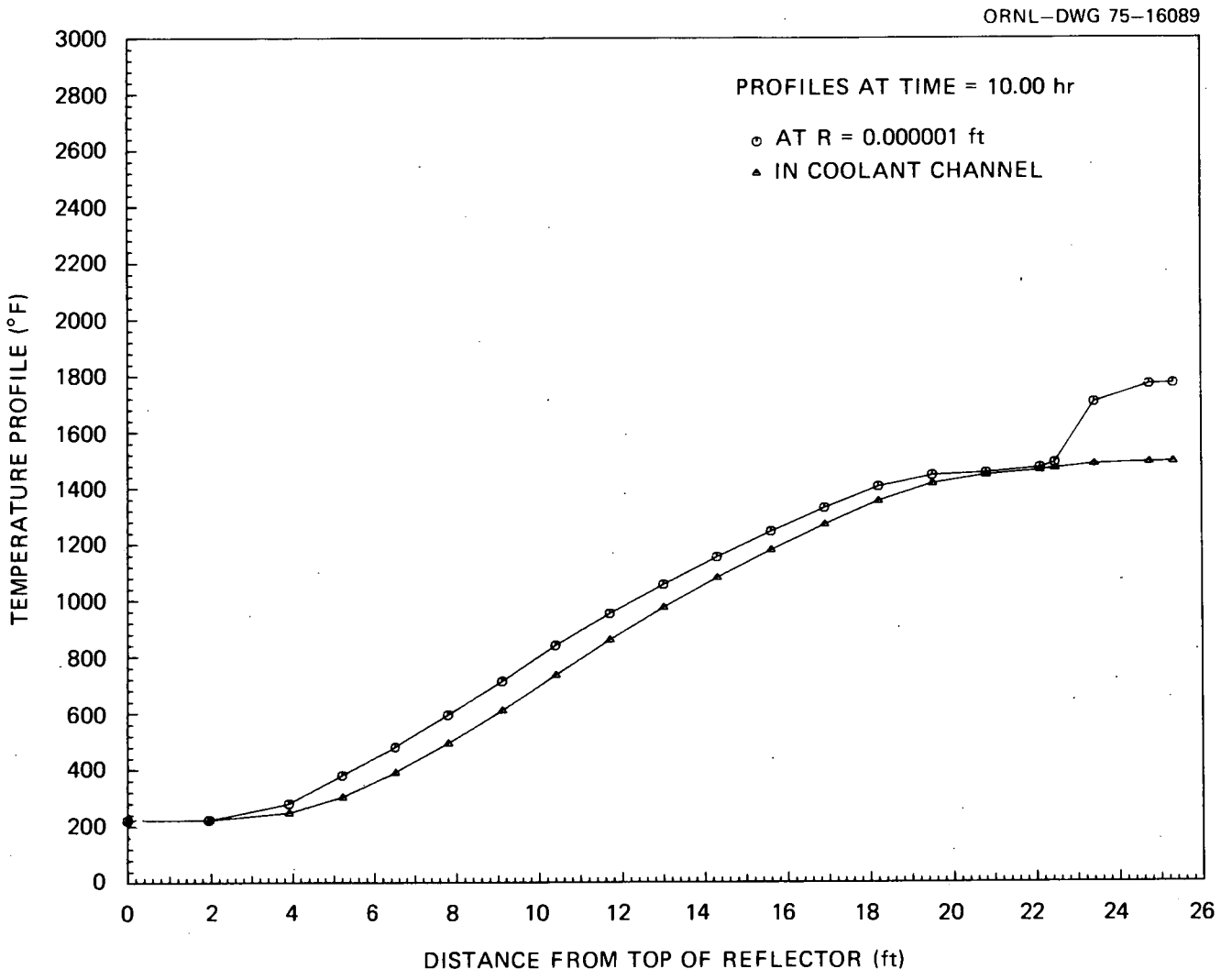

Fig. 15. Fuel and coolant profiles in the highest power refueling region ten hours after the specified DBDA in the Fort St. Vrain reactor.

CONCLUSIONS

Using information supplied by GAC for the total flow through the Fort St. Vrain reactor core following the depressurization accident, it was found that pressure drop in the primary circuit was less than the available head indicated by the circulator characteristic curves. The maximum torque required during the transient was 51 ft-lb. The apparent operating line for the system was very close to the projected stall curve for the circulators; however, GAC indicated that there was additional flow through the two by-pass loops that would move the operating point away from the stall line. The stall characteristics for this type of circulator are usually a fairly broad band and not a sharply defined line so that circulator operation can approach stall conditions without encountering an adverse situation.

The flooded steam generator appears quite capable of removing the heat from the circulating gas as indicated by the GAC tabulations. According to the GAC analysis, additional heat is removed from the circulating gas by the PCRV-liner cooling system. This effect was not included in the ORNL analysis.

A single-channel model was used to determine the temperatures in the reactor core during this transient. Use of this model implies that no allowance can be made for the removal of heat from the hottest region by conduction to an adjacent cooler region. It appeared that the limiting operating criterion during the transient was the exit gas temperature from the hottest region. Therefore, the ratio of the mass of graphite to the mass of fuel in the single-channel, or unit cell, was increased to represent the ratio that existed for an entire refueling region; this would be equivalent to neglecting the thermal lag due to the conduction of heat across the refueling region. This should result in a conservative value, or overestimate, for the exit gas temperature.

A maximum value for the exit gas temperature for operation with two circulators at 7000 rpm was approximately 2400°F. The exit temperature from the hottest region remained at a temperature greater than 2000°F over the period from 1.9 hr after depressurization to 6.5 hr after depressurization with the maximum temperature occurring at 4.0 hr. Mixing

with gas from cooler channels will decrease the gas temperature at the inlet ducts to the steam generators. The maximum average outlet temperature during this transient was found to be about 1900°F; this occurred at 3.5 hr after depressurization.

Based on the assumption that the mass flow through the core was directly proportional to circulator speed, it was estimated that a speed of 11,300 rpm would be required to keep the maximum temperature from the hottest region below 2000°F. A plot shows the maximum hot channel temperature and the average outlet temperature that occurs at the same time during the transient; both are shown as a function of circulator speed. Any assumed percentage mixing will indicate maximum temperatures at the duct as a function of circulator speed.

For the purpose of estimating the maximum fuel temperature during the transient, the conservatism involved in increasing the effective graphite in the single-channel model was removed. Thus, both inter-regional and intra-regional conduction were neglected. Even with this degree of conservatism, the maximum temperature found in the fuel during the transient was approximately 2600°F. The axial profiles in the graphite and fuel at various times during the transient are presented.

For comparison purposes, results from computations using the ORECA program are shown in the appendix to this report. The ORECA program represents only the active core of the reactor, and it is a lumped-node model. It does represent inter-regional conduction from the hot regions to the cooler neighbors. It has been written to predict the most probable values for the coolant and fuel temperatures, not necessarily the conservative values. These results agree very well with the values presented by GAC based on the RECA program.

APPENDIX

SIMULATION OF THE FSV DBDA USING THE ORECA CODE

S. J. Ball

The ORECA code is being developed at ORNL under the sponsorship of RSR. It is modeled after the GAC RECA code and, like RECA, predicts the three-dimensional transient thermal-hydraulic behavior of an HTGR during emergency shutdown conditions. Of the present versions of ORECA now in operation [Fort St. Vrain Reactor, 2000 MW(t) and 3000 MW(t)], the FSV has been developed in the most detail. A report now in preparation[18] describes the ORECA code in detail. The following is a brief summary of its characteristics and capabilities:

a) Each of the 37 refueling regions and 18 side reflector blocks are represented by 8 axial nodes. Six of the axial nodes in the refueling region represent the active core, one the top reflector, and one the bottom reflector and core support blocks. This results in a total of 440 nodes for the core simulation.

b) Coolant heat transfer coefficient calculations include the effects of changing flow regimes (turbulent-transition-laminar), and the effects of helium conductivity variations with temperature.

c) Present inputs include the total helium flow rate, pressure, and inlet temperature vs time, and the total reactor power input vs time which follows a typical scram curve. Axial and radial power peaking factors are input and assumed constant throughout the run.

d) The flow calculated for each channel is dependent upon friction losses, acceleration losses, buoyancy effects, and entrance/exit orifice pressure drops. Friction losses calculated are dependent on the flow regime.

e) Channel flows are calculated at each time step by an iterative scheme to solve for the overall core pressure drop which gives the proper total flow rate (within a specified error). Reverse flows are also accommodated.

f) Composite core and graphite reflector conductivity and specific heat are calculated as functions of temperature.

The FSV reactor conditions and assumptions used in the ORECA reference calculation of the DBDA are as follows:

a) Total core power = 878.3 MW, (842 = 100% power),

b) Power Density = $\left(\frac{878.3}{842}\right) \times 6.3$ kW/liter = 6.57 kW/liter,

c) Composite core specific heat $C_p = 0.28 + 7.33 \times 10^{-5}T$ Btu/(lb-°F) ,

d) Composite core conductivity $k = 2.5 + 4.5 \times 10^{-3}T$ Btu/(ft-hr-°F) ,

e) Composite core density $\rho = 90$ lb/ft^3,

f) Total core flow rate = 3,666,700 lb/hr = 61,112 lb/min,

g) 99% of total power in the active core = 869.5 MW,

h) 1% of total power in side reflector = 8.8 MW,

i) 96.33% of total flow through refueling regions = 3,532,132 lb/hr,

j) 3.67% of total flow through side reflectors = 134,568 lb/hr,

k) Total number of refueling regions = 31 @ 7 elements + 6 @ 5 elements = 35.286 equivalent 7-element regions,

l) Initial channel flow distribution: channel flow proportional to region peaking factor QR,

m) Heat transfer from side reflector blocks to core helium inlet temperature is included,

n) Accident conditions: At time = 0^+, the pressure drops from 703 psia to 12.3 psia, the net core flow drops to 0, and the reactor scrams. At time = 5 min, the core net flow and inlet temperature follow the GAC-supplied curves.

The results of the reference case ORECA simulation are shown in Fig. A.1, along with RECA predictions. It can be seen that the results of the two codes compare favorably. ORECA's peak core and maximum gas outlet temperatures are 2230 and 1950°F, respectively. In the previous calculations by ORECA, conservatively low fixed values of composite core C_p (0.33 Btu/lb°F) and k (10Btu/hr ft°F) were used, along with a model of the lower reflector and core support block which underestimated their effective heat capacity. This had resulted in peak core and maximum gas outlet temperatures of 2340 and 2255°F, respectively. It is felt that the present calculations are more realistic.

Several variations of the reference ORECA case were run in order to determine the sensitivity of the results to various model and parameter

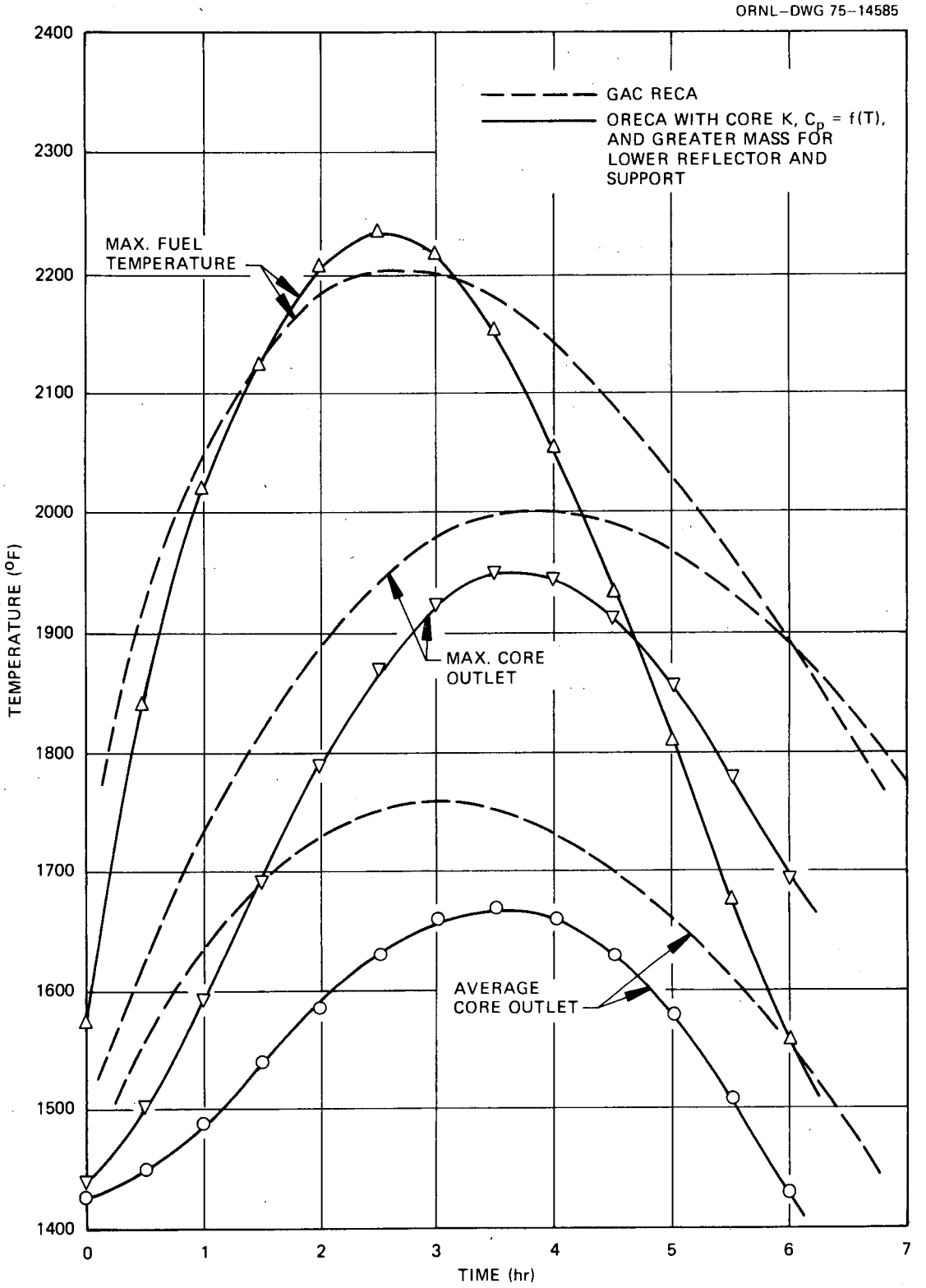

Fig. A.1. Analysis of the Fort St. Vrain depressurization accident using the ORECA computer program.

assumptions. Some experimental data indicate that the effective flow coefficients of orifices increase at very low flow rates; this would result in a more uniformly distributed flow. The effect was approximated by changing each of the region orifice factors K_i to be midway between the reference values and the overall average value. This change resulted in an additional 90°F increase in maximum core temperature and a 40°F increase in maximum coolant outlet temperature. The assumption of a 20% reduction in the values of core composite conductivity only increased the peak core and outlet temperatures by 30 and 40°F. When the value of $\overline{Q}/(\rho C_p)$ (the average region heatup rate with no cooling) was made 20% higher than the reference case, the calculated maximum core and outlet temperatures were 90 and 80°F higher.

A run was made in which the GAC-supplied values of emergency cooling helium flow vs time were reduced by 10%. This increased the peak core and outlet gas temperature by 80 and 50°F, and also delayed the times at which the peaks appeared.

A number of other variations were run which had only negligible effects on the calculated peak temperatures. These were:

1) The coolant channel "roughness" was changed from "very smooth" to that of wrought iron pipe.

2) The side-reflector heat conduction out to the outside annulus was neglected.

3) Refueling region 30 (with the highest radial power factor) was "swapped" with refueling region 15 so that it would no longer have a relatively cool side reflector neighbor.

4) The pressure drops due to the inlet orifice, entrance, and exit losses, which are lumped at the inlet for the reference case, were split appropriately between inlet and outlet.

5) The computation time interval, normally 5 min, was reduced to 1 min.

The major limitation of the present ORECA codes is their dependence on other sources (such as TAP and RECA calculations) for coolant flow and inlet temperature inputs. Further development of ORECA is planned to include models of the shutdown coolant flow and cooling system mechanisms

so that these inputs can be computed rather than specified. Further refinements are also planned for the modeling of the lower reflector and core support blocks.

REFERENCES

1. R. A. Clark, Letter to Public Service Company of Colorado, Docket No. 50-267 (Jan. 6, 1975).

2. R. F. Walker, Letter to Robert A. Clark, Docket No. 50-267 (Jan. 16, 1975).

3. R. A. Clark, Letter to Public Service Company of Colorado, Docket No. 50-267 (Feb. 7, 1975).

4. R. F. Walker, Letter to Robert A. Clark, Docket No. 50-267 (Feb. 28, 1975).

5. J. P. Sanders, Letter to R. A. Clark, Docket No. 50-267 (Mar. 21, 1975).

6. R. F. Walker, Letter to R. A. Clark, Docket No. 50-267 (July 8, 1975).

7. Gulf General Atomic Company, Operation and Maintenance Manual for the Fort St. Vrain 330-MW(e) HTGR Helium Circulators, Gulf-GA-A10349 p.24, (February 1972).

8. W. H. McAdams, Heat Transmission, 3d ed., p. 273, McGraw Hill, New York, 1954.

9. J. P. Sanders, HTGR Safety Studies, Quarterly Progress Report for Period Ending June 30, 1973, ORNL-TM-4741 (October 1974).

10. J. P. Sanders, HTGR Safety Studies, Quarterly Progress Report for Period Ending September 30, 1973, ORNL-TM-4739 (October 1974).

11. J. P. Sanders, HTGR Safety Studies, Quarterly Progress Report for Period Ending December 31, 1973, ORNL-TM-4738 (October 1974).

12. Delmarva Power and Light Company, Summit Power Station, Preliminary Safety Analysis Report.

13. Public Service Company of Colorado, Fort St. Vrain Nuclear Generating Station, Final Safety Analysis Report.

14. R. W. Schleicher, et al., An Analysis of HTGR Core Cooling Capability, Gulf General Atomic Company, Gulf-GA-A12504 (March 1973).

15. M. P. Wilson, Jr., Thermodynamic and Transport Properties of Helium, Gulf General Atomic, Inc., GA-1355 (January 1960).

16. G. R. Tully, Jr., Letter to J. P. Sanders, ORNL, Docket No. 50-267 (April 15, 1975).

17. Private communication with GAC personnel.

18. S. J. Ball, ORECA-I: A Digital Computer Code for Simulating the Dynamics of HTGR Cores for Emergency Cooling Analyses, ORNL-TM-5159 (In preparation).

Internal Distribution

1. J. L. Anderson
2. S. J. Ball
3. A. A. Brooks
4. J. P. Callahan
5. D. A. Canonico
6. H. P. Carter
7. J. C. Cleveland
8. T. E. Cole
9. J. H. Coobs
10. D. Costanzo
11. W. B. Cottrell
12. F. L. Culler
13. R. M. DeVault
14. G. G. Fee
15. M. H. Fontana
16. Uri Gat
17. G. E. Giles, Jr.
18. M. J. Goglia
19. R. W. Henderson
20. H. W. Hoffman
21. F. J. Homan
22. J. D. Jenkins
23-25. P. R. Kasten
26. A. L. Lotts
27. R. E. MacPherson/ J. A. Conlin
28. A. P. Malinauskas
29. Walter J. McCarthy
30. D. D. Paul
31. H. Postma
32. P. L. Rittenhouse
33. M. W. Rosenthal
34-50. J. P. Sanders
51. Dunlap Scott
52. Myrtleen Sheldon
53. I. Spiewak
54. J. R. Tallackson
55. John J. Taylor
56. D. B. Trauger
57. W. D. Turner
58. G. D. Whitman
59. W. J. Wilcox
60. ORNL Patent Office
61-62. Central Research Library
63. Document Reference Section
64-68. Laboratory Records Department
69. Laboratory Records Department (RC)

External Distribution

70. Director, Division of Reactor Licensing, USNRC, Washington, D.C. 20555
71. Director, Division of Technical Review, USNRC, Washington, D.C. 20555
72-81. Assistant Director for Reactor Safety, Division of Technical Review, USNRC, Washington, D.C. 20555
82-92. Chief, Gas Cooled Reactors Branch, Division of Reactor Licensing, USNRC, Washington, D.C. 20555
93. Chief, Reactor Systems Branch, Division of Technical Review, USNRC, Washington, D.C. 20555
94. Chief, Core Performance Branch, Division of Technical Review, USNRC, Washington, D.C. 20555
95-96. Director, Office of Nuclear Regulatory Research, USNRC, Washington, D.C. 20555
97. Assistant Director, Advanced Reactor Safety Research, Division of Reactor Safety Research, USNRC, Washington, D.C. 20555
98. Chief, Experimental Gas Cooled Reactor Safety Research Branch, Division of Reactor Safety Research, USNRC, Washington, D.C. 20555
99. Director, Division of Reactor Research and Development, ERDA, Washington, D.C. 20545
100-101. Office of Reactor Safety Research Coordination, ERDA, Washington, D.C. 20545

102. Assistant Director, Gas Cooled Reactor Projects, Division of Reactor Research and Development, ERDA, Washington, D.C. 20545
103. Assistant Director, Reactor Safety, Division of Reactor Research and Development, ERDA, Washington, D.C. 20545
104. Chief, Gas Reactor Safety Branch, Division of Reactor Research and Development, ERDA, Washington, D.C. 20545
105. Director, Research and Technical Support Division, ERDA, ORO
106. Director, Reactor Division, ERDA, ORO
107-133. Technical Information Center, ERDA, Oak Ridge
134. W. H. Beach, EGCRSRB, Division of Reactor Safety Research, USNRC, Washington, D.C. 20555
135. R. E. Ireland, Division of Technical Review, USNRC, Washington, D.C. 20555
136. R. Lobel, Division of Technical Review, USNRC, Washington, D.C. 20555